Muthanna Journal of Engineering and Technology, Vol. (10), Issue (1), (Year) 2022

Muthanna Journal of Engineering and Technology

Website: https://muthjet.mu.edu.iq/

Research paper, Short communication, Review, Technical paper

Assessment of Flexible Pavement Behavior Under Dynamic Earthquake Loading

Mariam M. Hussein[a], Mohammed Y. Fattah[b] and Miami M. Hilal[c]

[a] Assistant lecturer, Laser & Optoelectronic Engineering Department, Alkut university College, Iraq. Email: maryam.m.hussain@alkutcollege.edu.iq

[b] Professor, Civil Engineering Department, University of Technology, Baghdad, Iraq. Email: myf_1968@yahoo.com

[c] Assistant Professor, Civil Engineering Department, University of Technology, Baghdad, Iraq. Email: mmh_com@yahoo.com

DOI:10.52113/3/eng/mjet/2022-10-01/01-08

Abstract

Through cushioning the pressures caused from high traffic at prior asphalt, a reinforcing interlayer delays the formation of cracks at bitumen overlay. Experimental effort comprises of laboratory testing that better known behavior of sand as a subgrade and its impact on flexible pavement and base-course layer during earthquakes. The sand layer was 600 mm thick; the base was 200 mm thick, and the asphalt layer was constructed as a panel with dimensions of 300*300*50 mm, representing surface. These layers are put to the test with varied earthquake loading frequencies of 0.5, 1, and 1.5 Hz. Experiments were divided into two sections: one without geogrid and the other with geo-grid at center of -base and among base and sand. It was discovered that the frequency of ground movement causes cracks in the asphalt layer, which increases with shaking frequency and reduces with geogrid installation.

Keywords: *Pavement, geogrid reinforcement, dynamic, stresses, displacements.*

1. Introduction

There are two sorts of elements that influence the performance of flexible pavements: exterior and inner factors. Pavement deterioration is influenced by external elements such as traffic loads, the environment, and styling concerns.

Loads, as well as the environment, cause pavement to deteriorate over time. According to the most basic pavement structural model, each person load causes a specific degree of irreversible harm. This harm accumulates along the pavement's life, and when it extends a certain higher value, the pavement is said to have reached the end of its usable life of service.

Whole pavement analysis ways are based on static or moving loads and do not account for inertia effects caused by dynamic loads. The main effects of earthquakes are shaking and ground rupture, which cause more or less severe damage to houses and other stiff structures. The magnitude of local impacts is determined by a complicated mix of the earthquake's magnitude, distance from the epicenter, and local geological and geomorphological characteristics, which can enhance or diminish wave propagation.

Holder and Andreae (2004) evaluated the benefits of geo-grid reinforcement using data from the falling weight deflectometer test (FWD). The analysis revealed that a control section (unreinforced section) is essential for determining the benefit of geogrid reinforcement.

Using integrated geogrid and woven geo-grid, Jeon (2008) investigated the test technique for evaluating the long-term performance of the different types of geo-grids. In comparison to the integrated geogrid, the experience conclusions showed that the knitted geo-grid had a high strength to over term distortion. Long term creep deformation was estimated to be between 60 and 65 percent of ultimate loading. The optimum values in the woven geogrid that satisfy the creep requirement.

The dynamic behavior of the multilayer pavement subgrade system was investigated through Zheng et al. (2012). To better understand dynamic conduct of a piece of a pavement subgrade, tests were conducted to measure stresses and irreversible continual distortion at various deepness. Transportation and reversal matrices (TRM) procedure was utilized in conjunction with the physical model to generate public solutions for stresses and displacements of layered system subjected to dynamic double circular loads at its roof.

Jebur et al. (2021) conducted experiments in which the road layers were subjected to a harmonic dynamic load of 10-and 15-kN with two frequencies of 0.5-and 1-Hz. A stress gauge sensor was used to measure the vertical stress in the road layers. It was discovered that by raising the frequency and load amplitudes in situation of a reinforcing geogrid in center of the base course, stress lowers (23-42). Stress and vertical displacement decrease with increasing frequency and-load capacity in situation of a supporting layer in middle of base. With increased frequency and loads, a minimal drop in stress and vertical displacement could be achieved while geogrid was put among sand and base layer.

The goal of this study is to investigate the effects of various dynamic para-meters on pavement layer response, such as load frequency and base thickness, as well as the impact of earthquake loads on stress convey in asphalt layers and the effect of different tremor load values and frequencies on induced strains, displacements, and stresses between flexible pavement layers.

2. Experimental Work

2.1 Materials

Natural cohesionless soil (sand) used as a sand layer in study was obtained from Iraq's Karbala area. It has undergone a number of physical tests, and it has been classified as (SP-SM) soil by USCS (ASTM D2487-17) and AASHTO (A-STM D3282-15) classification systems. The base course was chosen from the Al Nibaee quarry, located north of Baghdad. This type of base is commonly used as a layer in flexible pavement construction. Crushed aggregates came from the Al-Nibaay quarry. Tests (angularity, sieve analysis, flat and elongation, toughness through (Los Angeles abrasion), specific gravity, soundness, and equivalent sand (clay content) were utilized to determine the physical and chemical parameters, as display in Table 1. The findings of the sieve analysis are shown at Table 2.
One grade of asphalt was used in this project, which is (40 -50), thus according Al-Daurah Refinery's classification Table 3 lists the physical characteristics of asphalt.

Table 1. Physical properties of selected aggregate

Laboratory Test		AS-TM Designation and Specification	Result			
Specific gravity	Coarse aggregate	ASTM C 127	Sieve size (mm)	Apparent Gs	Bulk Gs	Abs. %
			12.5	2.674	2.651	0.32
			9.5	2.591	2.585	0.09
			4.75	2.582	2.570	0.18
	Fine aggregate	ASTM C 128	4.74-0.075	2.642	2.615	0.48
Angularity for Coarse aggregate		ASTM D 5821 Min 95%	97%			
Soundness for coarse aggregate		ASTM C 88 10-20% Max	3.2%			
Equi-valent sand (clay-content)	Natural (< # 4)	AST-M D2419 Min 45%	84.5%			
	Crushed (< # 4)		89.6%			
Flat & elongation aggregate	Flat	ASTM D 4791 Max 10%	0.9%			
	Elongation		2.5%			
Toughness by -(los Angeles abr-asion	Aggregate-size < 25 mm	ASTM C131 30% Max	21.3%			

Table 2. Sieve analysis of base

Sieve size (mm)	Cumulative Wt. retained (g)	% Retained	Pa-ssing %	Specification limits
37.5	0.0	0.0	100.0	100.0
25.0	942.0	1.7	98.3	80 – 100
19.0	6978.0	12.5	87.5	
12.5	17860.0	32.1	67.9	50 – 80
4.75	29408.0	52.8	47.2	30 – 60
0.425	44642.0	80.1	19.9	10 – 30
0.075	51104.0	91.7	9.3	5 – 12
Pan	-	-	-	-

Table 3. Physical properties of asphalt cement

Test	Result	SCRB Specifications
Penetration (25°C, 100 g, 5 sec)	47	40-50
Ductility (25°C, 5 cm/min)	110	≥ 100
Softening point (ring & ball).	53	50-60
Flash and fire point	261, 264	≥ 232
Loss on heating (163°C, 50 gm, 5h)%	0.07	< 0.75
Specific gravity asphalt	1.049	---
Rotational Viscosity	0.6425@135 °C 0.164@165°C	---

* SCRB State Corporation for Roads and Bridges in Iraq.

2.2 Pavement layer preparation

Slabs of compacted asphalt mixture were used to imitate the pavement layer. The asphalt slab was constructed using a steel model with dimensions of 300-mm wide, 300-mm longitudinally, and 50 mm thickness. To achieve the desired dimensions, approximately 10522.4-grams of asphalt mix was mixed at the optimum asphalt content (5.25 percent), then evenly applied to the oiled steel mold with a hot plated spatula, and the surfaces were levelled. To achieve the identical Marshall specimen's bulk density of 2.32 kg/m3 and requisite thickness of 50 mm, a com-pression static stress of 100-kN was applied for 6 minutes at 154-°C. As shown in Figure 1, each slab was left for overnight before being taken of the mold and wrapped in polyethylene to protect its properties from the impacts of the environment.

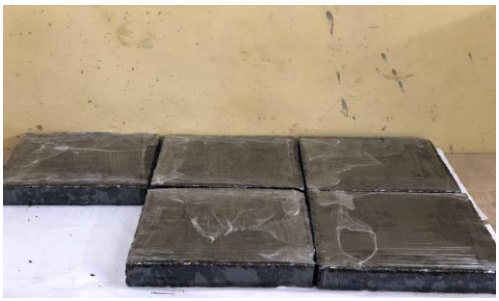

Figure 1. Asphalt slab model**.**

2.3 Thickness of the model layers

Several research linked to this study determined the thickness of the chosen layer; for example, the thickness of the subgrade was chosen as 600 mm based on the work of Al-Utabi (2011), Reddy (2013), and Teama (2014), and the base-layer was 200 mm thick, and the asphalt layer was 50- mm thick. Figure 2 shows profile of the pavement layers.

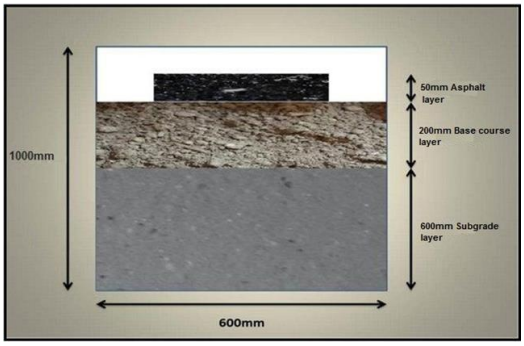

Figure 2. Profile of model layers.

2.4 Geo-grid reinforcement

In all tests, geogrid used was type-SS2 manufactured by QM-OF-CO (Quality Material for Oil Field). The geogrid sheet was used in multiple tests; however, it was replaced when it be-came noticeably over stressed or damaged.

2.5 Shaking machine

A shaking table, which is vital laboratory equipment that simulates the loading that occurs during dynamic excitation as in an earth-quake, was utilized to replicate earthquake excitation in the laboratory. The type of loading can be harmonic, random, or genuine seismic movement, for example. The basic four components of the shaking table appliance are the shaking tab-le foundation, electrical motor-and AC-drive, steel-box, and damping system.

Al-Recaby et al., (2016) layout and manufactured the shaking table shown in Figure 3. The steel box is mounted on an L-shaped sheet and link-ed with a 15-mm-diameter screw bolt. Inner dimensions of the steel box are (800 800 1000) mm.

Figure 3. The shaking-box**.**

The pressures were calculated using tactile-pressure-sensors with a 10 kPa capacity. By detecting the volume of displacement across a number of elements and converting it to a distance, a la-ser displacement sensor was used to measure the distance between the sensor and item. Two sensors are fastened on opposing sides of the sample panel to monitor horizontal displacement.

2.6 Unreinforced models

The bed of sand is placed in the steel container before earthquake is applied, and the first sensor is positioned 50 mm beneath the surface of the sand. The base layer was then placed on top of the subgrade, compacted by hand with a steel hammer, and levelled. The second sensor was buried 50 mm beneath the base course layer's middle. Then, as indicated in Figure 4, the asphalt layer slab specimen was placed on the base course, the third sensor was positioned precisely beneath the asphalt layer, and a 900*900 mm steel plate was placed on the asphalt layer.

Figure 4. Pavement layers in unreinforced model.

2.7 Reinforced models

The SS2 geogrid layer was placed on top of sand layer after the bed of sand soil was prepared. Then, as previously noted, the base-course-layer was-laid with compaction, and the asphalt slab was placed on top of it. The processes were then repeated with the geogrid in a various location, once in center of base and once above the-base-layer. initial sensor was installed 50-mm below sand surface, another sensor-was installed 50-mm below center of base-course layer, and the third sensor was installed exactly beneath the asphalt-layer.

2.8 Crack measurement

It was developed a high-quality microscope for measuring crack widths in concrete members, masonry walls. An adjustable lamp unit powers device, and the image is focused by rotating a knob. The eyepiece scale can be rotated to match the direction of the crack or pitch being investigated. Figure 5 depicts the crack meter measurement instrument. To measure the width of the cracks in the asphalt layers, place the gadget on the crack and measure the width. The following standards were used to measure the cracks in the asphalt layer, as illustrated in Figure 5: 1. Magnification: x 40 2. Measuring range: 4 mm 3. Subdivision: 0.02 mm 4.

Figure 5. Crack meter device.

3. Results and Discussion

Under dynamic-load of 0.5,-1,-1.5-Hz frequency, the-vertical stress transferred to the sand subgrade, base course, and asphalt layer is shown in Figure 7. Clearly, as seen in these graphs, the stress level rises as the frequency rises. In the frequency 1.5 Hz, there is a rapid change in stress compared to the frequencies 0.5-and 1-Hz, where there is no change in-these two cases. The highest tension observed at 1.5-Hz is higher than-the maximum stress recorded at 0.5-and 1-Hz.

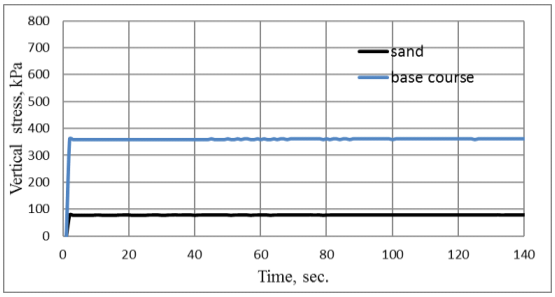

a. Base and subgrade

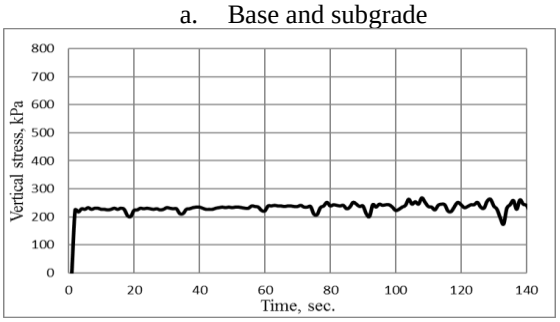

b. Asphalt

Figure 6. Variation of vertical stress in road layers under frequency 0.5 Hz.

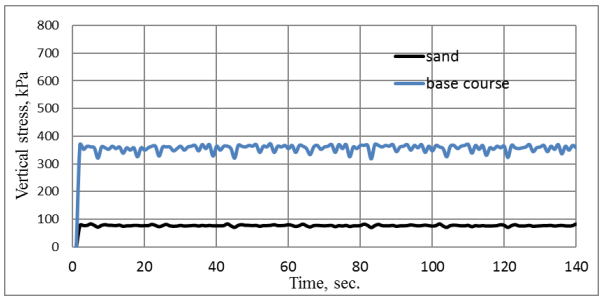

a. Base and subgrade.

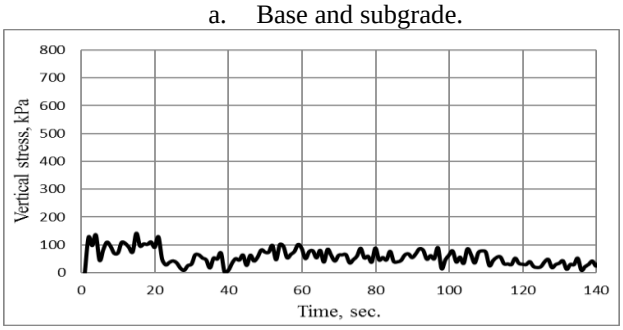

b. Asphalt.

Figure 7. Varia-tion of ver-tical str-ess in-road-layers un-der freq-uency 1 Hz.

The horizontal displacement observed under-dynamic-loading conditions is shown in Figures 8 and 9. The largest displacement is re-corded in frequency 1 Hz, while the lowest-value of displacement is recorded in frequency 0.5-Hz, according to the data in the figures. Because of the quick movement, the displacement oscillates; nevertheless, after about 80 seconds, the displacement approximates a stable state. The maximum displacement in frequency 1-Hz is 80 percent more than-the maximum dis-placement in frequency 0.5, and the maximum displacement in frequency 1-Hz is 12.6 percent greater than the maximum displacement in frequency 1.5-Hz. This means that at 1-Hz, the greatest horizontal displacement occurs.

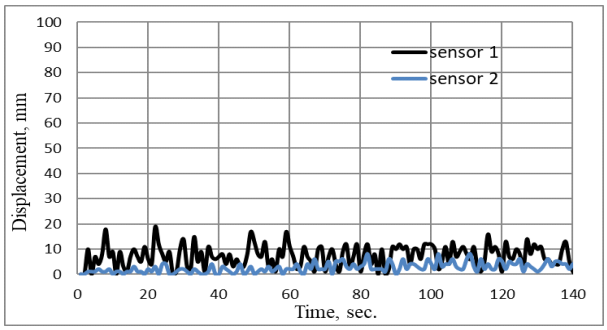

Figure 8. Variation of horizontal displacement at road-layers below frequency 0.5 Hz.

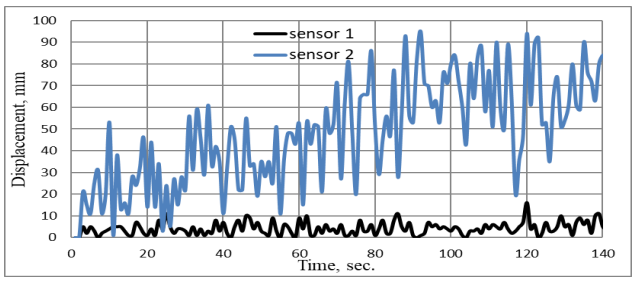

Figure 9. Variation of horizontal displacement in road-layers below frequency 1 Hz.

Figures 10 and 11 shows the vertical-stress imparted to the sand-base, base-course, and asphalt-layer-under different frequencies of dynamic load. According to the figures, when the geo-grid is-placed at middle of the-base-layer, stress in the sand-layer-from the base-course-layer is reduced for frequencies of 0.5, 1, and 1.5 Hz. The maximum stress occurs when geo-grid is at-center of base-course layer and frequency is-1 Hz.

The deformed geogrid has a membrane force with a vertical component that-resists applied-loads, providing vertical support-to-underlying soil mass subjected to-loading. The membrane effect is a term used to describe how geogrid works. According to Fattah et al., the interlocking effect of geogrids occurs when the soil is interlocked through the apertures (openings) between the longitudinal and transverse ribs Fattah et al (2017a).

According to the figures, the maximum stress with the geo-grid in the middle of the base layer occurs at frequency 0.5-Hz, which is 9.1% lower than the unreinforced model at the same frequency, and stress at frequency 1 Hz-with geo-grid in

middle of base layer are 42.3 percent higher than the un-reinforced model at the same frequency. Maximum stress in the model with geo-grid at the center of the base-course is just 0.2 percent higher than in the unreinforced model at 1.5 Hz.
After 500 cycles, Fattah et al. (2017b) found that the influence of load frequency on the settlement ratio is nearly constant. In general, the influence of load frequency on the settlement ratio for reinforced cases is relatively minimal, ranging between 0.5–2%, when compared to the unreinforced case.
Without geogrid, the soil is generally granular and functions as a flexible layer. When the geogrid is introduced, the soil and geo-grid overlap, causing the soil mass to work as a single unit, increasing the inertia force and increasing the stress in the layer. Furthermore, because the geogrid stiffness is high, the stresses increase, especially when loading frequency at the layers is raised, except when the geogrid is added at center of the base layer at a frequency of 0.5 Hz, when the stress decreases.

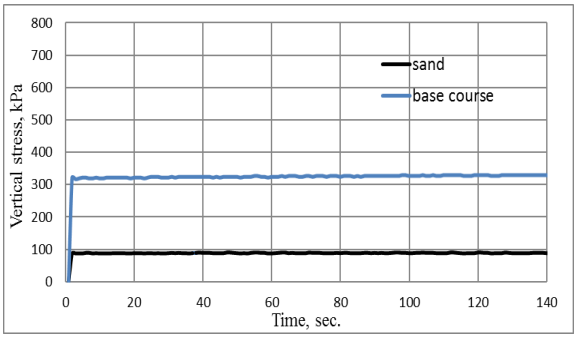

a. Base and subgrade

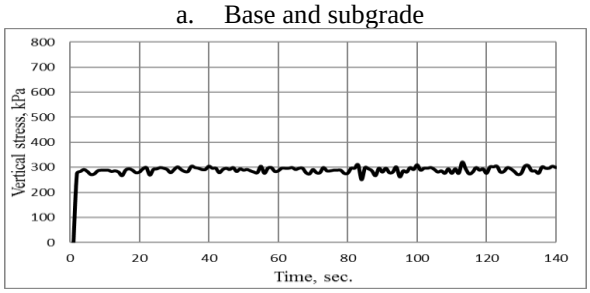

b. Asphalt

Figure 10. Variation of vertical stress in road-layers under frequency 0.5-Hz, SS2 geogrid at the center of base layer.

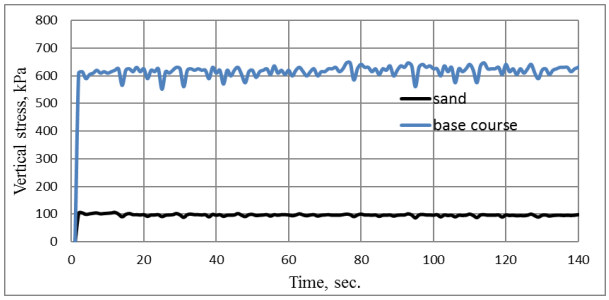

a. Base and subgrade

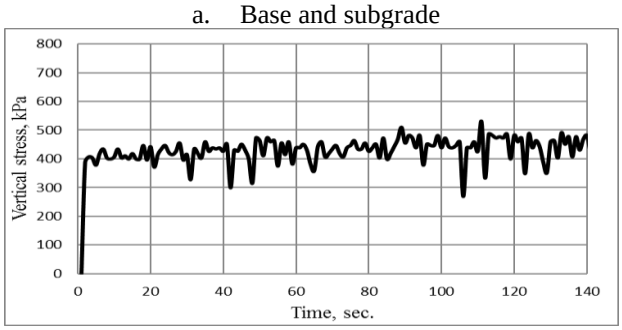

b. Asphalt

Figure 11. Variation of vertical stress in road-layers under frequency 1 Hz, SS2 geogrid at center of base layer.

The crack width of the asphalt layer results for the unreinforced and reinforced models has been measured as shown in Figure 12. According to Table4, the crack that occurs while the geo-grid is positioned between the base course and subgrade occurs at frequency 0.5-Hz and is 14.2 percent lower than-that of the unreinforced model at the same frequency, and the crack that occurs at frequency 1 Hz with geo-grid between the base-course and sand is about 50 percent lower than that of the unreinforced model at the same frequency. The fracture in the model-with geogrid between the base course and the sand revealed same value as unreinforced model at 1.5 Hz.

Figure 12. Measuring of cracks at asphalt layer.

Table 4 Show crack measurements in layers.

Case-study	Frequency (Hz)	Crack width (micron)	Crack position
Without geogrid	0.5	175	edge
	1	150	Cen-ter
	1.5	200	edge
Geo-grid at the center of the base	0.5	150	edge
	1	50	edge
	1.5	200	Cen-ter
geogrid among base and subgrade	0.5	150	Cen-ter
	1	75	edge
	1.5	200	edge

4. Conclusions

The following conclusions can be drawn based on the results of the model tests conducted on the various factors to consider the influence of earthquake on the road layers:

1. 1. The frequency of ground movement causes a crack in the asphalt layer, which increases with shaking frequency and reduces with geogrid placement.
2. The largest crack width is 250 microns when the-geo-grid is in the center of the base-course-layer and occurs at a frequency of 1.5-Hz.
3. The maximum crack width is 200-microns when geogrid is placed among base course and sand layer at a frequency of 1.5 Hz.
4. Utilizing the geo-grid is advantaged to boundary the tensile strains at the below of asphalt which-have been utilized as a design criterion to block fatigue cracking.
5. Stress in-sand subgrade layer is less than that in base and asphalt layers when the geo-grid is installed among base course and subgrade sand layer for two thicknesses of base-layer-300 and 200-mm.

References

[1] Al-Utabi, A. I. K., (2011), "An approach in improving unpaved roads overlying soft clay soils using geogrid", M.Sc. thesis, College of Engineering, Al-Mustansiriyah University, Iraq.

[2] ASTM D2487 – 17, "Standard Practice for Classification of Soils for Engineering Purposes (Unified Soil Classification System)", American Society for Testing and Materials.

[3] ASTM D3282 – 15, "Standard Practice for Classification of Soils and Soil-Aggregate Mixtures for Highway Construction Purposes", American Society for Testing and Materials.

[4] Fattah, M. Y., Aladili, A. S., Yousif, H. F., (2017), "Investigation of Reinforced Sub-base Layer on Saturated Expansive Subgrade Soil under Cyclic Loading", International Journal of Earth Sciences and Engineering, Vol. 10, No. 3, 604-615, DOI:10.21276/ijee.2017.10.0319.

[5] Fattah, M. Y., Aladili, A. S., Yousif, H. F., (2017), "Behavior of Reinforced Sub-base Layer on Dried Expansive Soil under Cyclic Loading", Journal of Earth Sciences and Geotechnical Engineering, Vol. 7, No. 3, 23-49.

[6] Holder W. H. and Andreae, J. (2004), "Geogrid Reinforcement to Reduce Pavement Section Thickness: A Case Study‖ ASCE, Conference Proceedings Paper, Geotechnical Engineering for Transportation Projects (GSP 126) Reston, Va., pp. 1006-1024.

[7] Jebur, F. F., Fattah, M. Y., Abduljabbar, A. S., (2021), "Function and Application of Geogrid in Flexible Pavement under Dynamic Load", Engineering and Technology Journal 39 (08) (2021) 1231-1241. http://doi.org/10.30684/etj.v39i8.1771.

[8] Jeon, H.-Y., (2008): "Theoretical approach of long-term behaviors of geogrids", the 12th International Conference of International Association for Computer Methods and Advances in Geomechanics (IACMAG), 1-6 October, Goa, India.

[9] Reddy, L., (2013), "Influence of subgrade condition on rutting in flexible pavements- an experimental investigation", International Journal of Civil Engineering and Technology, vol. 4, Issue 3, pp. 30-37.

[10] Teama, Z. T., (2014), "Suitability of dune sands subgrade beneath flexible pavement structure under repeated loads", M.Sc., thesis, College of Engineering, Al-Mustansiriyah University, Iraq.

[11] Zheng, L., Lin, Y. H., Wan-peng, W. and Ping, C., (2012), "Dynamic stress and deformation of a layered road structure under vehicle traffic loads: Experimental measurements and numerical calculations", Soil Dynamics and Earthquake Engineering, vol. 39, pp. 100-112.